




# Chloride Molten Salt Electrolysis Enables Integrated and Energy-Efficient Process for NdFeB Magnet Fabrication

B.P. HOLCOMBE,<sup>1,4,5</sup> A. VILLALOBOS,<sup>1</sup> N.S. SINCLAIR,<sup>1,5</sup>  
E.L. LANTZ,<sup>2</sup> D.R. HOFFMAN,<sup>2</sup> E. KIM,<sup>2,5</sup> A.A. BAKER,<sup>2,5</sup>  
J. CUI,<sup>3,5</sup> B.Z. CUI,<sup>3,5</sup> A.E. LONG,<sup>4</sup> and R. AKOLKAR<sup>1,4,5,6</sup> 

1.—Department of Chemical and Biomolecular Engineering, Case Western Reserve University, Cleveland, OH 44106, USA. 2.—Lawrence Livermore National Laboratory, Livermore, CA 94550, USA. 3.—Ames National Laboratory, Ames, IA 50011, USA. 4.—Galvanix Incorporated, Cleveland, OH 44110, USA. 5.—Critical Materials Innovation Hub, Ames, IA 50011, USA. 6.—e-mail: RNA3@case.edu

Rare-earth elements (REEs) have been identified by NATO, the USDOE, and USGS as critical materials, i.e., materials which have significant demand yet pose supply-chain risks. Many of the existing processes for separations, metallization, and final parts production used across the REE supply chain involve energy intensive steps. For example, neodymium (Nd or NdPr) is produced using oxyfluoride electrolysis of  $\text{Nd}_2\text{O}_3$ , which requires hydrofluoric acid to produce a key electrolyte component ( $\text{NdF}_3$ ) and generates undesired perfluorocarbon (PFC) gases. Such challenges make securing a resilient supply chain for NdFeB permanent magnets in countries like the United States prohibitively difficult. Here, we propose a chloride-based MSE process that circumvents these challenges, delivering high-purity NdPr from a  $(\text{NdPr})\text{Cl}_3$  feed from upstream REE separations. This eliminates environmentally-damaging steps of oxalate or carbonate precipitation and calcination, and enables superior production rates due to greater solubility of  $(\text{NdPr})\text{Cl}_3$  in chloride melts compared to  $\text{Nd}_2\text{O}_3$ . We show that CMSE generates high-purity NdPr (99.4 wt.%) while being energy-efficient ( $\sim 6$  kWh/kg-Nd). NdPr from CMSE was used to fabricate a NdFeB magnet with an excellent maximum energy product ( $> 40$  MGOe), comparable to commercially available NdFeB magnets. This establishes CMSE as a leading approach for integrated, energy-efficient NdFeB magnet production.

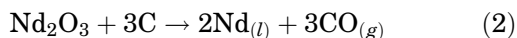
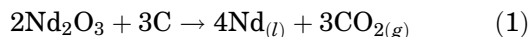
## INTRODUCTION

Nd (or NdPr) metal is a critical component of NdFeB permanent magnets, which are found in hard disk drives, many ubiquitous energy technologies such as EVs, defense equipment, and health-care devices. Demand for NdFeB magnets, and thus for Nd or NdPr metal, is expected to increase over the coming decades, yet the overwhelming majority of this metal is mined and refined overseas, creating a fragile domestic supply chain.<sup>1</sup> The US currently mines about 15% of the world's rare-earth oxides,

but, until recently, has very few processing facilities: separating the oxides, converting the oxides into high-purity metal, and converting the metal into final usable parts such as NdFeB magnets. A significant roadblock in the “oxide-to-metal” conversion step is the permitting requirement in the US necessary to operate the widely-practiced and industrially-accepted oxyfluoride molten salt electrolysis process. This is due to the emission of considerable PFCs as anode gases in addition to CO and  $\text{CO}_2$ . The treatment of PFCs requires incineration and HF formation which can be a significant health hazard to operators. The oxyfluoride process dissolves  $\text{Nd}_2\text{O}_3$  in a  $\text{NdF}_3\text{-LiF}$  (90:10 by mass) molten salt at  $1050^\circ\text{C}$ , and produces Nd (or NdPr)

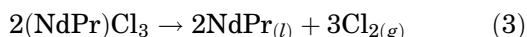
(Received May 26, 2025; accepted September 15, 2025)

metal at the cathode in liquid form. CO and CO<sub>2</sub> are the primary gaseous products from the reaction of Nd<sub>2</sub>O<sub>3</sub> with C from the anode:<sup>2</sup>



CF<sub>4</sub> and C<sub>2</sub>F<sub>6</sub> are also formed as undesirable anode gases when mass transport limitations are imposed due to the low solubility of Nd<sub>2</sub>O<sub>3</sub> (4 wt.%) and the high anode current density (~ 1 A/cm<sup>2</sup>). This problem is exacerbated when significant blockage of the anode surface occurs from adsorbed gas bubbles (predominantly PFCs) via the so-called “anode effect.”<sup>3,4</sup> In addition, the consumable nature of the C anode requires frequent replacement and eventually necessitates shutdown of operation, making the oxyfluoride process intrinsically semi-batch.

As an alternative to oxyfluoride electrolysis, chloride molten salt electrolysis (CMSE) uses the electrolysis of rare-earth element (REE)-containing chloride molten salts to evolve chlorine gas (Cl<sub>2</sub>) as the anode product and REE metal (e.g., Nd or NdPr) as the cathode product. The chlorine evolution reaction does not consume the carbon anode, rendering the anode largely inert during electrolysis so long as the electrolyte remains relatively dry. Furthermore, efforts to develop dimensionally-stable anodes (DSA) have begun, where the DSA serves as both a catalyst to Cl<sub>2</sub> evolution and a protective coating for graphite should residual water or dissolved oxides contact the anode.<sup>5–7</sup> Use of a DSA or an inert anode for evolving Cl<sub>2</sub> facilitates a fully continuous operation as electrolysis cells will not require shutdown for anode replacement, making the process operationally attractive.



Laboratory-scale efforts have been attempted to electrowin Nd from NdCl<sub>3</sub> but these have resulted in low coulombic efficiency (~ 40%) owing to poor atmospheric control, high levels of back reaction of the metal with dissolved Cl<sub>2</sub> gas, and loss of Nd<sup>2+</sup> intermediates to redox-shuttling.<sup>8–12</sup> However, moderate temperature electrowinning efforts producing solid Nd (or a liquid alloy with a suitable alloying cathode) have shown that improved coulombic efficiency (> 85%) is possible by controlling the current density, electrolyte composition, and metal polarization.<sup>5,6,13,14</sup> Additionally, a key benefit of chloride molten salts is that they typically have lower viscosity and thus higher ionic conductivity compared to fluoride molten salts at the same temperature, allowing for reduced voltaic losses.<sup>15</sup> This combination of improved current and voltage efficiencies allows for reduced energy usage during metallization.

An unappreciated yet major cost advantage of CMSE is that certain processing steps become redundant when a Nd or NdPr chloride mixture, e.g., NdCl<sub>3</sub> or (NdPr)Cl<sub>3</sub> is the feedstock. For example, aqueous NdCl<sub>3</sub> streams are produced in conventional upstream separations from which Nd<sub>2</sub>O<sub>3</sub> is extracted via oxalate or carbonate precipitation and calcination. If the chloride form is made the direct input to CMSE electrolysis, the energy, cost and environmental footprint associated with precipitation and calcination can be completely eliminated as shown in green (proposed route) in Fig. 1. Here, we show how the CMSE process, when practiced at 1050°C, can deliver high-purity NdPr metal (99.4 wt.%) while enabling very high current densities (> 15 A/cm<sup>2</sup>). The high rate is a result of the high solubility of (NdPr)Cl<sub>3</sub> in chloride melts. Coulombic efficiency of metal production and associated cell voltage characteristics support high energy-efficiency (~ 6 kWh/kg-Nd for CMSE versus 8 kWh/kg-Nd for oxyfluoride electrolysis). The Nd metal obtained via CMSE was used to fabricate a NdFeB magnet with a superior maximum energy product of > 40 MGOe, comparable to commercial grade N45 NdFeB magnet. These results establish CMSE as a promising alternative for an upstream–midstream integrated, energy-efficient and cost-competitive NdFeB magnet production process.

## MATERIALS AND METHODS

### Electrolysis Reactor for Nd Metal Production

All the electrochemical experiments were performed in cells made of graphite crucibles placed inside a furnace under an Ar blanket (Airgas, industrial grade) at 1050°C (see Fig. 2). Electrolysis was performed galvanostatically where the cathode current density was held constant around 15 A/cm<sup>2</sup>. The concentric cylinder arrangement of electrodes comprised of a 0.3-cm-diameter molybdenum rod as the cathode (McMaster Carr). The anode was a flat bottom graphite crucible (graphitestore.com, fine grain extruded, inner diameter = 8.89 cm) which acted as the cell and its exterior was coated in firebrick cement to prevent oxidation of the carbon. Not shown in Fig. 2 is a pyrolytic boron nitride crucible (99.3% purity; MSE Supplies) placed underneath the cathode in which the electrowon Nd or NdPr metal was collected and kept insulated from the graphite anode. The electrolyte for NdPr production experiments comprised of 64 wt.% CaCl<sub>2</sub> (> 99% purity; Lab Alley), 20 wt.% as-dried (NdPr)Cl<sub>3</sub>, 11 wt.% LiF, and 5 wt.% CaF<sub>2</sub>. The choice of CaCl<sub>2</sub> is because of its low vapor pressure particularly when fluoride additives are added. The (NdPr)Cl<sub>3</sub> was provided by MP Materials in an aqueous solution form, and was first dried at 80°C in air, then vacuum dried for 1.5 h at 200°C at nominally 0.1-Torr pressure.<sup>16</sup> Semi-quantitative thermogravimetric analysis (TGA) was performed on a Discovery TGA55 under UHP nitrogen with a

## Chloride Molten Salt Electrolysis Enables Integrated and Energy-Efficient Process for NdFeB Magnet Fabrication

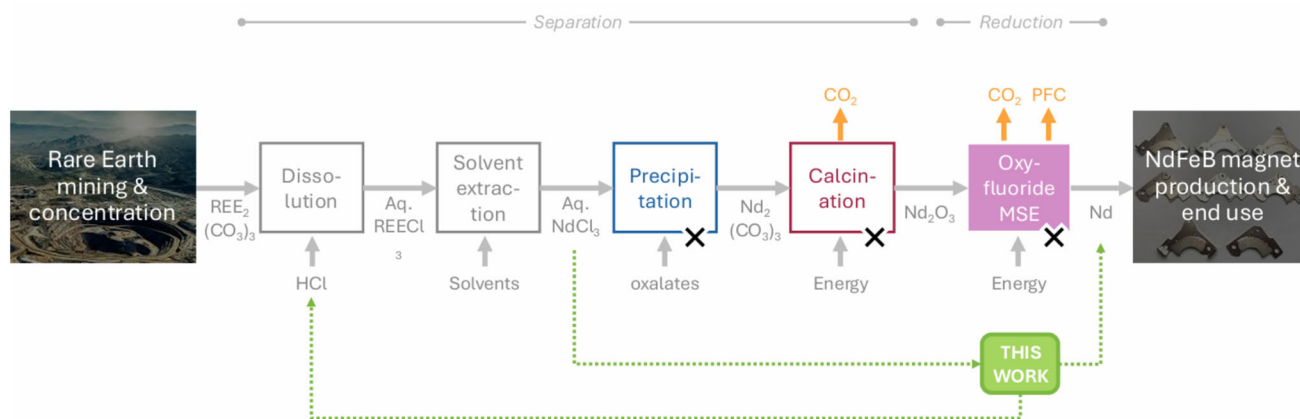


Fig. 1. Widely-practiced industrial process (gray arrows) for mine-to-magnet involving energy-intensive unit operations and associated environmental impacts, notably PFC emissions. In the proposed integrated CMSE approach, (NdPr)Cl<sub>3</sub> aqueous stream generated in upstream REE separations is the direct input to electrolysis, which eliminates precipitation and calcination unit operations and provides Nd metal for direct fabrication of sintered NdFeB magnets. Additionally, CMSE circumvents use of costly NdF<sub>3</sub> salt needed for oxyfluoride MSE, which itself requires HF for its production (Color figure online).

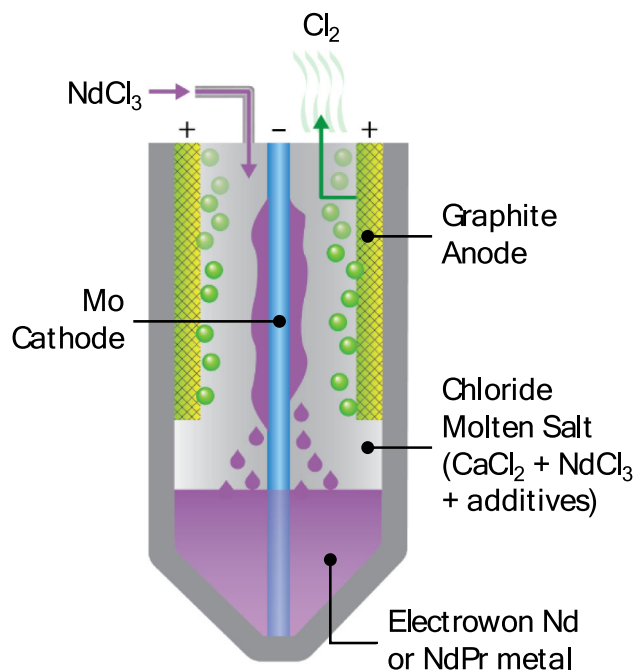


Fig. 2. Schematic of the CMSE reactor used in this work. Reactor was operated at 1050°C at around 15 A/cm<sup>2</sup> cathode current density for about an hour, generating Nd metal at a coulombic efficiency of about 70%. Input (NdPr)Cl<sub>3</sub> was obtained by drying an aqueous (NdPr)Cl<sub>3</sub> stream from upstream REE separations processing. Not shown here is a BN crucible, which was used for metal collection and its insulation from the anode.

ramp rate of 100°C/min. TGA showed that there were approximately 3 H<sub>2</sub>O molecules for every (NdPr)Cl<sub>3</sub> after the 80°C drying step, and approximately 1 H<sub>2</sub>O molecule per (NdPr)Cl<sub>3</sub> after the vacuum drying step based on mass loss at the first stable plateau (~ 275°C) and assuming that the NdCl<sub>3</sub> is predominant stable species at this temperature (Fig. 3). It is likely that most if not all of the

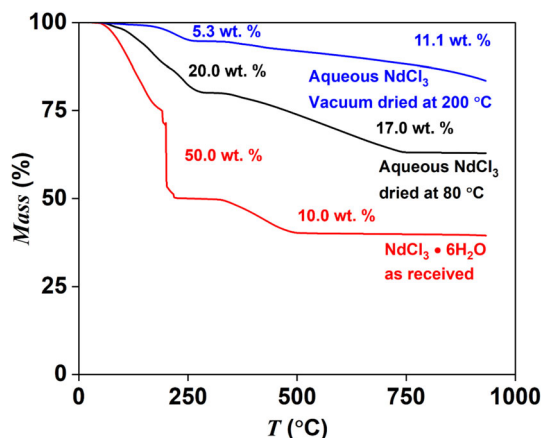


Fig. 3. Thermogravimetry data showing mass loss due to dewatering of aqueous (NdPr)Cl<sub>3</sub> as received (red) and that post-vacuum drying at 200°C (blue), and post-drying at 80°C (black). The 200°C vacuum-dried (NdPr)Cl<sub>3</sub> has the least amount of water, represented by only a ~ 16% loss in mass during TGA and indicating that the starting material for electrolysis had a composition of roughly (NdPr)Cl<sub>3</sub>•1H<sub>2</sub>O. The percentage mass losses represent mass change from the starting temperature to ~ 255°C, and then from ~ 255°C to 933°C (final temperature) (Color figure online).

remaining H<sub>2</sub>O molecules are driven off by the high temperatures and inert atmosphere during electrolysis. The salt was not characterized for the formation of NdOCl as the Cl<sub>2</sub> headspace promotes the stability of NdCl<sub>3</sub> compared to NdOCl,<sup>17</sup> and NdCl<sub>3</sub> and NdOCl form a stable liquid phase at temperatures exceeding ~ 750°C.<sup>18</sup> After electrolysis, the bath was allowed to cool to 800°C, which caused the electrowon metal to solidify. The crucible was then extracted out of the molten salt using crucible tongs. The electrowon metal was then placed inside a VAC Nexus II glovebox (< 10 ppm H<sub>2</sub>O, < 1 ppm O<sub>2</sub>) and abraded using sandpaper and a wire brush to clean off residual salts on its surface. Note here that



“Nd” and “NdPr” are used interchangeably as (NdPr)Cl<sub>3</sub> feedstocks routinely contain PrCl<sub>3</sub>, which also undergoes electrolysis given that Nd and Pr have similar electrochemical properties, and magnet fabrication is largely insensitive to the Pr content of Nd.

### Electrowon Metal Characterization

O, H, and N contents in electrowon Nd (or NdPr) metal were determined through combustion analysis with a LECO-836 series gas analyzer. To prevent unwanted oxidation, ~ 0.8-g pieces of NdPr were crimped into Ni crucibles in an Ar-filled glovebox with < 0.1 ppm O<sub>2</sub>. The sealed crucibles were transferred to the analyzer under Ar and quickly loaded into the inert measurement chamber to minimize contamination. Five measurements were performed to minimize uncertainty, and calibration using material with known impurity levels was conducted immediately before and after the measurements.

Single aliquots of samples and process blanks were analyzed for major, minor, and trace elements with a Thermo Scientific iCAP triple quadrupole-inductively coupled plasma-mass spectrometer (TQ-ICP-MS). Samples were dissolved in 30-mL Savillex Teflon vials in 8 M HNO<sub>3</sub> and heated on a hotplate at 120°C for 16 h. After visually inspecting the samples to ensure complete dissolution, the solutions were diluted in 4 M HNO<sub>3</sub> with 18.2 MΩ ultrapure water. Three acid process blanks were prepared alongside the samples. ICP-MS analysis was run in kinetic energy discrimination mode with helium as the collision gas to mitigate the effect of lighter REE polyatomic interferences on heavier REE measurements. A total of 54 elements were measured. Standards and samples were prepared gravimetrically. Fully quantitative analyses using a linear calibration curve based on certified external standards in a matching Nd matrix were performed.

### Magnet Fabrication and Characterization

Electrowon NdPr from CMSE was first purified by induction melting at 1200–1300°C for 1–2 min before its use in magnet fabrication. The NdFeB-sintered magnet (composition was Nd<sub>24</sub>Pr<sub>8</sub>Fe<sub>66</sub>-Co<sub>1</sub>B<sub>1</sub>, expressed as wt.%) made from the purified CMSE NdPr is referred to as the ‘CMSE’ magnet. NdFeB magnets were fabricated via the conventional powder metallurgical route. Ingot alloys were first prepared by arc melting the constituent materials: Fe (99.97%) and Co (99.5%) (both Thermo Scientific Chemicals), purified NdPr from CMSE, and FeB alloy (Shieldalloy Metallurgical). Coarse-grained NdFeB alloy flakes were produced using strip casting onto a copper wheel rotating at 2 m/s. These strip-cast flakes underwent hydrogen decrepitation (HD) at room temperature in 4.7 atm of H<sub>2</sub> gas for 5 h, resulting in coarse alloy powders. The powders were then loaded into a ball milling jar

containing cyclohexane, inside a dry N<sub>2</sub>-filled glove box. Low-energy ball milling was carried out for 11 h using a 16:1 ball-to-powder ratio on a roller mill. After milling, the powder was dried in the glove box by decanting the cyclohexane. The resulting fine powders consisted of single-grain particles with an average size of approximately 3.6 μm. The dried powder was compacted in a rubber die and magnetically aligned under a 9-T pulse field. Magnetic alignment was performed using a pulse magnetizer (9487; Magnetic Instrumentation). The aligned powders were then cold-isostatically pressed (CIP) at 500 MPa using a CIP die set (CIP500-DIE; MTI) under a hydraulic press (V75-15-PX; Wabash MPI). The compacts were sintered at 1080°C for 1.5 h, followed by post-annealing at 900°C for 0.5 h, and subsequently at 580°C for 1 h.

An N45-grade reference magnet was also fabricated using the same procedure described above. The only difference was that the starting material was a commercially available N45-grade NdFeB alloy powder. This magnet had composition [Nd<sub>24.05</sub>Pr<sub>7.68</sub>Ga<sub>0.18</sub>Cu<sub>0.15</sub>Co<sub>1.02</sub>B<sub>0.93</sub>Fe<sub>balance</sub> (wt.%)] comparable to that of ‘CMSE’ magnets as analyzed by inductively coupled plasma-atomic emission spectroscopy.

After final pulse magnetization, the magnetic properties of the samples were measured using a closed-loop hysteresis graph with a maximum applied field of 2 T (Laboratorio Elettrofisico AMH-500). The tested samples were cylindrical, with dimensions of approximately 11 mm (diameter) and 11 mm (height), where the height corresponds to the magnetization direction (M). The magnet density was determined using the Archimedes method.

### Techno-Economic Analysis

A detailed unit-level techno-economic analysis (TEA) model was created.<sup>19–23</sup> For the CMSE process (Fig. 1, green), the model included equipment for drying of the aqueous (NdPr)Cl<sub>3</sub> feedstock, electrolysis, and capture of the generated Cl<sub>2</sub> gas. Cl<sub>2</sub> was valued as a commodity rather than recycling it back into upstream separations. The comparison to the conventional oxyfluoride process was made by eliminating drying and Cl<sub>2</sub> capture from the model, replacing them with estimates for precipitation and calcination, and adapting various input parameters to be more representative of oxyfluoride electrolysis.<sup>1</sup> Production of 1000 tonnes per annum was assumed.

For the TEA model, reasonable assumptions were made for a variety of process parameters (e.g., plant lifetime, utilization, electrolysis cell size, operating voltage, residence times, efficiencies, waste rates; key model parameters are provided below). These process parameters were used to calculate detailed process flow and equipment sizing. Equipment sizing was input into equipment exponential cost correlations and utilities requirements which were

further refined with CPI inflation and materials of construction correction factors.<sup>19,20,24</sup> A standard engineering factorial method was used to translate equipment costs into fully loaded fixed capital (e.g., installation, electrical, instrumentation, design, and engineering).<sup>22</sup> Factors based on fixed capital were used to approximate maintenance, insurance, and land, rent, and property taxes. Direct labor was derived using an exponential cost curve for labor hours based on process volume which was converted to cost with a standard hourly wage.<sup>23,25</sup> Other labor-related expenses (e.g., supervision, payroll) were derived using factors based on direct labor expense.<sup>22</sup> Finally, other operating costs were based on the material flow analysis used to size the equipment and a variety of market price assumptions as discussed below.

When adapting the model to the conventional oxyfluoride electrolysis (Fig. 1), many of the cost assumptions from the recent DOE magnet supply chain analysis were leveraged.<sup>1</sup> The inclusion of a consumable graphite anode contributes US\$4.20/kg-NdPr based on a consumption rate of 0.2–0.4 kg-C/kg-Nd. Smith et al. also include capital costs for the electrolysis cell that were incorporated into the TEA model.<sup>1</sup> For precipitation and calcination steps, published materials consumption rates (e.g., carbonate and natural gas) were used.<sup>26</sup>

## RESULTS AND DISCUSSION

### CMSE Operation, Process Efficiency, and Metal Purity

The input for CMSE was (NdPr)Cl<sub>3</sub> obtained from drying an aqueous (NdPr)Cl<sub>3</sub> feedstock (from upstream separations) sourced by MP Materials. Figure 4a shows an image of the dried chloride. The assay provided with the sample indicated an Nd/Pr ratio of 3.5:1 and a metals basis purity of 99.9 wt.%. The dried (NdPr)Cl<sub>3</sub> was added at 20 wt.% concentration with the other salt components and heated to 1050°C, then subjected to electrolysis at ~15 A/cm<sup>2</sup> for ~1 h. The recorded cell voltage ( $V_{\text{cell}}$ ), as shown in Fig. 4b, was about 7.8 V. This cell voltage comprises several overpotentials, namely the ohmic overpotential ( $\eta_{\Omega}$ ), the activation overpotentials at the anode and cathode ( $\eta_a$ ), and the mass-transport overpotentials due to concentration polarization ( $\eta_c$ ). Given that the thermodynamic potential for electrolyzing (NdPr)Cl<sub>3</sub> is about 3 V, the measured cell voltage suggests the sum total of all overpotentials to be about 4.8 V. A predominant portion of this voltage loss is due to the resistance in the wiring, contact resistance between electrical junctions, and the electrolyte resistance between the cathode and anode. Activation and concentration polarization are typically small, given the superior kinetics (very high exchange current density,  $i_0$ ) and diffusion properties (very high diffusivity of Nd<sup>3+</sup> species given the low viscosity of the CaCl<sub>2</sub> melt, leading to very high limiting

current density,  $i_L$ ).<sup>2,5,6</sup> After electrolysis, the metal was weighed and the coulombic yield  $\varepsilon$  was calculated using:

$$\varepsilon = \frac{mnF}{ItM} \quad (4)$$

where  $m$  is the mass (g) of the NdPr metal recovered,  $t$  is the time of electrolysis (s),  $I$  is the total applied current,  $M$  is the molar mass of NdPr, and  $n$  is the number of electrons transferred (= 3). The coulombic yield achieved in this work was ~70%, which is a significant improvement compared to similar laboratory-scale efforts in oxyfluoride electrolysis (~50%).<sup>27</sup> The increased efficiency is the result of suppressed parasitic and back reactions enabled by the electrolyte composition, high current density (which lowers Nd<sup>2+</sup> formation), and polarization of the formed NdPr metal.<sup>2,5,6</sup> Current yields at industrial scales (1–5 kA) for the oxyfluoride process tend to be higher, and a similar trend is observed in the Hall–Héroult process for primary aluminum production.<sup>28–32</sup> Thus, it is likely that, as the CMSE process is scaled, improvements to current yield will be realized, leading to further lowering of the energy consumption (in kWh/kg), given as:

$$\text{energy} = \frac{(V_{\text{cell}})nF}{M\varepsilon(3600)} \quad (5)$$

where  $V_{\text{cell}}$  is the cell voltage, and all other values have the same meaning as previously defined. The specific energy consumption (energy) calculated based on the measured cell voltage was ~6 kWh/kg. Figure 4c shows an image of the NdPr metal (44 g) that was recovered from the boron nitride crucible post-electrolysis and cleaned (using sandpaper) to remove a thin layer of residual salts on its surface. This metal was analyzed using ICP-MS and combustion analysis (LECO) and was found to have a bulk purity of 99.4 wt.%, with the major impurities shown in Fig. 4d. The Al impurity likely came from an Al<sub>2</sub>O<sub>3</sub> sheath used to reduce the cathode surface area, and was subsequently removed from the apparatus for the NdPr samples generated for magnet fabrication. The Mo impurity content comes from the NdPr being in contact with the Mo cathode. The Fe impurity likely came from the anode gas (Cl<sub>2</sub>) attacking a stainless-steel containment vessel forming FeCl<sub>3</sub> in the head space, which could then get absorbed into the molten bath. Mg impurity was traced back to an assay from the supporting electrolytes. These metallic impurities can be addressed through process optimization and are expected to reduce in fraction as the process is scaled-up. Ultimately, the purity of the as-electrowon metal from CMSE is comparable to that produced via the conventional oxyfluoride process (> 99 wt.%), with low (< 0.05 wt.%) O levels being particularly important for NdFeB magnet performance. The low N

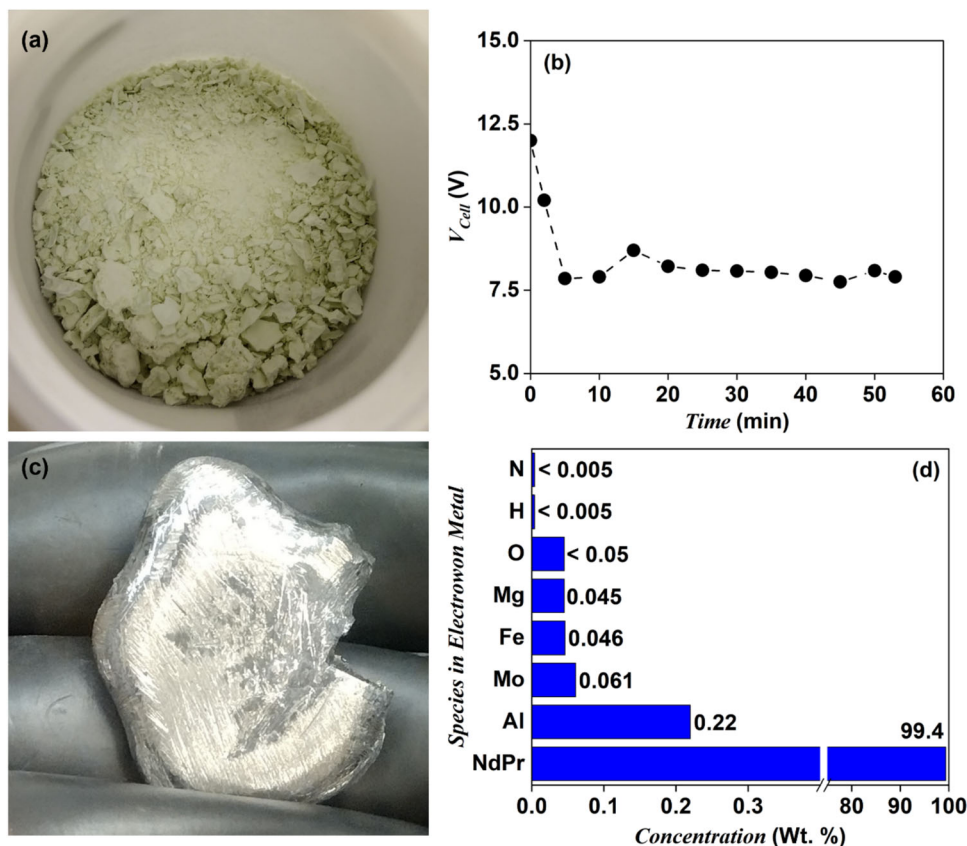


Fig. 4. (a) Image of  $(\text{NdPr})\text{Cl}_3$  obtained after low-temperature drying of an aqueous  $(\text{NdPr})\text{Cl}_3$  feedstock from upstream separations; (b) cell voltage during CMSE of the dried  $(\text{NdPr})\text{Cl}_3$  in  $\text{CaCl}_2$  electrolyte at  $1050^\circ\text{C}$  as a function of time shows a steady-state value of  $\sim 7.8$  V; (c) an image of 44 g NdPr metal collected after CMSE for 1 h at  $\sim 15$  A/cm $^2$ ; (d) LECO and ICP-MS analysis reveal 99.4 wt.% pure NdPr metal with very low levels of impurities.

content indicated no significant impurity incorporation from the boron nitride crucible. Chloride levels were undetectable too per EDS analysis.

### NdFeB Magnet Fabrication and Property Characterization

As shown in Fig. 5, the NdFeB magnet produced using CMSE NdPr (blue curve) using the above fabrication procedure (see Methods section) demonstrated excellent magnetic properties with a remanence  $B_r = 13.1$  kG, intrinsic coercivity  $H_{ci} = 11.1$  kOe, maximum energy product  $BH_{\max} = 40.8$  MGOe, and density  $\rho = 7.54$  g/ml. These properties are comparable to the N45 grade reference magnet (black curve,  $B_r = 13.6$  kG,  $H_{ci} = 14.4$  kOe,  $BH_{\max} = 43.8$  MGOe, and  $\rho = 7.54$  g/ml). These findings represent the first successful demonstration of NdFeB-sintered magnets fabricated using NdPr electrowon via CMSE, achieving magnetic performance comparable to commercial-grade magnets. The slightly higher impurity level of CMSE NdPr metal ( $\sim 99.4$  wt.% purity), especially its increased oxygen content, is likely the main cause of the reduced coercivity in the sintered magnet compared with those made using commercial NdPr metal ( $\geq 99.5$  wt.% purity) for Nd-Fe-B magnets.

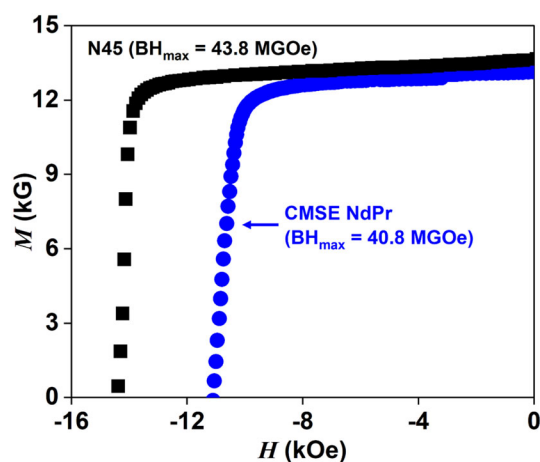


Fig. 5. Demagnetization curves of NdFeB magnet using CMSE NdPr (blue) and a representative N45 grade magnet (black). Both magnets were fabricated using the same procedure as described above. Starting material for N45-grade magnet was commercially available HD coarse NdFeB alloy powder (Color figure online).

### Techno-Economic Analysis of an Integrated Process Flow Enabled by CMSE

As discussed above, existing supply chains for NdPr metal for permanent magnets leverage multi-stage solvent extraction to isolate individual rare



earths (Fig. 1).<sup>33</sup> Solvent extraction is followed by conversion from a REE metal chloride stream to a metal oxide through precipitation and calcination. This generates the  $\text{Nd}_2\text{O}_3$  feed for traditional oxyfluoride electrolysis. Alternatively, our CMSE process eliminates the need for precipitation and calcination steps in favor of a simple drying process to prepare the  $(\text{NdPr})\text{Cl}_3$  feedstock. Additionally, the CMSE process as shown here exhibits superior coulombic efficiency (70%), very high metal purity (99.4 wt.%), and now (through magnet fabrication, Fig. 5) also competitive magnetization properties of an NdFeB magnet. A comparison of the estimated costs of NdPr conversion (oxyfluoride MSE versus CMSE) is shown in Fig. 6. Assumptions for techno-economic analysis are listed in Table I. Roughly, a > 2.5 times reduction in cost is noted, due to various factors as discussed below.

Comparing the oxyfluoride and CMSE cost stacks, the most significant cost benefit (\$4.20/kg) comes from elimination of the consumable graphite anode and instead replacing it with an inert anode (note: for CMSE, graphite itself is inert as long as the electrolyte is water-free).<sup>30</sup> Other inert anodes are also being developed for CMSE.<sup>5</sup> Savings from labor (\$0.6/kg-Nd) are due to “continuous” metal production instead of a manual semi-batch incumbent oxyfluoride process that requires regular replacement of consumable graphite anodes and frequent process stoppages to remove the center cathode and ladle out the produced molten NdPr metal. CMSE is assumed to be continuous as magnesium electrolysis cells operate continuously for multiple years at a time before cell rebuild is necessary.<sup>30</sup> Savings from

the supporting electrolyte (\$0.4/kg-Nd) come from predominant makeup of costly  $\text{NdF}_3$  (> 85 wt.% of the bath at > \$180/kg) in the oxyfluoride MSE process. Use of  $\text{NdF}_3$  is required due to the high melting point and low solubility of the  $\text{Nd}_2\text{O}_3$  feedstock.  $\text{NdF}_3$  is also partly consumed over time to produce PFCs and must be replaced.<sup>1</sup> For CMSE, the  $(\text{NdPr})\text{Cl}_3$  feedstock melts below the melting point of Nd metal and has very high solubility in chloride melts. As a result, much cheaper, easily available salts can be used (e.g.,  $\text{CaCl}_2$ ) as the supporting electrolyte which are less viscous and have high conductivities, resulting in lower ohmic losses. Though the CMSE electrolysis step itself is around 25% more energy efficient (lower cell voltage and improved coulombic efficiency), this benefit is partially offset by the added drying step. CAPEX savings (\$0.1/kg-Nd) are achieved via both increased cathodic current densities and improved utilization (driven by the shift from semi-batch to continuous processing) which are in part offset by the additional equipment for drying and  $\text{Cl}_2$  capture.<sup>31,32</sup> The elimination of precipitation and calcination steps contributes an additional \$1.5/kg-Nd and \$1.1/kg-Nd of savings, respectively. Of the “all else” costs in Fig. 6 (e.g., wasted feedstock, maintenance, insurance) assumed to be similar between the two methods, wasted feedstock is the most significant contributor at ~\$2/kg-Nd. Though it remains to be demonstrated, by avoiding manual ladling for metal removal and eliminating graphite anode replacements in favor of a more continuous process, there is opportunity for further upside of the CMSE process via maximized material yield. Note that feedstock transportation costs are assumed similar for both  $\text{NdCl}_3$  and  $\text{Nd}_2\text{O}_3$ , though in practice it is likely that the CMSE process will be deployed on-site with separations in order to make use of chlorine byproduct and the returns from vertical integration.

Additional upside in CMSE is the avoidance of costs associated with mitigation of the generated PFCs. Though some studies argue that, by deviating from the most efficient metal-making operating conditions, some PFC mitigation can be achieved,<sup>34</sup> it is anticipated that some sort of plasma arc thermal oxidizer would be required to fully eliminate PFC emissions at the cost of generating highly corrosive HF.<sup>35</sup> Either route (less optimal operating conditions and stringent monitoring, or plasma arc thermal oxidization) will contribute additional costs for the incumbent oxyfluoride technology, if deployed responsibly. However, reliable cost estimates were difficult to obtain at this time as it is not the standard practice to mitigate the PFCs produced. At present, NdPr metal is typically produced in open cells, venting any CO and PFCs produced directly to the atmosphere, making an outsized contribution to environmental damage.<sup>33,36</sup>

Overall, Fig. 6 shows that utilizing process intensification for feedstock material in CMSE has an

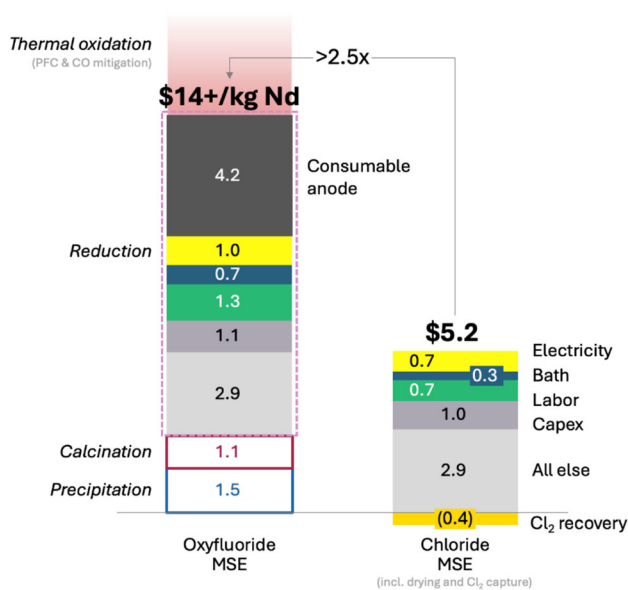


Fig. 6. Estimated costs of NdPr metal production in the US, comparing the oxyfluoride route (conventional process) with the proposed CMSE route integrated with upstream  $(\text{NdPr})\text{Cl}_3$  feedstock. Assumptions are provided in Table I.

**Table I. Parameters used for techno-economic analysis**

Parameter	Units	Oxyfluoride MSE	Chloride MSE (CMSE)	Note	Reference
<i>Operating Scale</i>	TPY	1000	1000	Aligned to MP Materials present separation capacity	37
Plant lifetime	Year	15	15	Reduced versus 20-year standard assumption given use of high-temperature media	
Utilization	%	72	85	Base assumption of 85% for continuous process; Oxyfluoride reduction based on assuming 1 h per shift lost to metal removal and 1 of every 25 days lost to anode replacement	38
NdCl <sub>3</sub> concentration	M	n.a.	> 0.8	Based on commercial samples post-solvent extraction	
Temperature	°C	1050	1050	Above the melting point of NdPr metal (1021°C)	
Current	A	3,000	3,000	Standard industry sizing, though up to 10 kA have been reported	1
Voltage	V	10	6	CMSE bath is less viscous, has higher concentrations, and a consistent inter-electrode distance due to non-consumable anode	33
Feedstock material yield	%	97	97		33
Current yield (coulombic efficiency)	%	70	80		33
Supporting electrolyte loss rate	%/month	2	600	Approximation for CMSE to allow for increased volatility of chloride salts; Note that any volatilized salts are likely to be captured and returned to the cell in addition to already being far cheaper than the NdF <sub>3</sub>	1
<i>Pricing</i>					
Electricity	\$/MWh	71.50	71.50	For Ohio	39
Natural gas	\$/GJ	6.37	6.37	For Ohio	39
Nd <sub>2</sub> O <sub>3</sub>	\$/kg	54.40	n.a.		40
NdCl <sub>3</sub>	\$/kg	n.a.	36.52		
NdF <sub>3</sub>	\$/kg	181.82	n.a.		1
CaCl <sub>2</sub>	\$/kg	n.a.	0.22		41
Cl <sub>2</sub>	\$/kg	n.a.	0.58		21

n.a. not available.

approximate \$9/kg-Nd cost reduction associated with it predominantly driven by the non-consumable nature of the anode, and the removal of precipitation and calcination steps needed for the oxyfluoride MSE. Further, the significant enhancement of current density allows for a similar improvement in space-time yield ( $Y$ ):

$$Y = \frac{i\varepsilon M\sigma}{nF} \quad (6)$$

where  $\sigma$  is the specific electrode surface area (cm<sup>2</sup>/cm<sup>3</sup>) defined as the electrode surface area divided by the fluid volume of the electrochemical reactor,  $i$  is the cathode current density (A/cm<sup>2</sup>), and the rest of the values have their previously defined meanings.

The space-time yield effectively describes the productivity of the reactor normalized to time and volume, and is a proxy for the capital expense required to start a plant of a desired volume. The high current densities for CMSE compared to the oxyfluoride process help enhance  $Y$  such that a much smaller reactor (smaller electrodes) can be utilized to make the same amount of NdPr, especially given that  $\varepsilon$  is already high (70% for CMSE versus 50% for oxyfluoride MSE). The combination of enhanced reaction rates, excellent current yield, and the enhanced margin provided from upstream integration collectively makes CMSE a techno-economically attractive choice.



## CONCLUSION

This work provides a feasibility proof-of-concept for an integrated, energy-efficient process for NdPr metallization. Aqueous (NdPr)Cl<sub>3</sub> obtained from upstream REE separations was subjected to drying, and the dried (NdPr)Cl<sub>3</sub> was electrolyzed in a CaCl<sub>2</sub>-containing chloride melt (CMSE) at 1050°C and very high current densities (~15 A/cm<sup>2</sup>). Resulting NdPr metal was electrowon at high efficiency (70 %) and exhibited very high purity (99.4 wt.%). The metal was successfully fabricated into a sintered NdFeB magnet with excellent properties, e.g., a maximum energy product of 40.8 MGOe, comparable to commercial-grade NdFeB magnets. Techno-economic analysis revealed the potential for reducing metal production costs from > \$14/kg-Nd (for the incumbent oxyfluoride process deployed in the US) to ~ \$5/kg-Nd for upstream-integrated CMSE. Given these advantages, the CMSE approach exhibits potential for being disruptive to NdPr metal production especially in geographies where considerations of energy, cost and environmental-friendliness are key drivers.

## ACKNOWLEDGEMENTS

This work was performed under support from the Critical Materials Innovation Hub, an Energy Innovation Hub funded by the U.S. Department of Energy (DOE), Office of Energy Efficiency and Renewable Energy, Advanced Materials & Manufacturing Technologies Office. Portions of this work were performed by LLNL under Contract DE-AC52-07NA27344. The authors gratefully acknowledge MP Materials for providing aqueous (NdPr)Cl<sub>3</sub> samples.

## CONFLICT OF INTEREST

On behalf of all authors, the corresponding author states that there is no conflict of interest. We disclose that some of the authors (Holcombe, Akolkar, Long) are stockholders or consultants in the company Galvanix Inc. Additionally, some of the authors (Holcombe, Akolkar, Sinclair) are inventors of intellectual property licensed by CWRU to Galvanix Inc. and cited within this paper.

## OPEN ACCESS

This article is licensed under a Creative Commons Attribution 4.0 International License, which permits use, sharing, adaptation, distribution and reproduction in any medium or format, as long as you give appropriate credit to the original author(s) and the source, provide a link to the Creative Commons licence, and indicate if changes were made. The images or other third party material in this article are included in the article's Creative Commons licence, unless indicated otherwise in a credit line to the material. If material is not included in the article's Creative Commons licence

and your intended use is not permitted by statutory regulation or exceeds the permitted use, you will need to obtain permission directly from the copyright holder. To view a copy of this licence, visit <http://creativecommons.org/licenses/by/4.0/>.

## REFERENCES

1. B.J. Smith, M.E. Riddle, M.R. Earlam, C. Iloje, D. Diamond. *Rare Earth Permanent Magnets: Supply Chain Deep Dive Assessment*. U.S. Department of Energy (2022).
2. R. Akolkar, *J. Electrochem. Soc.* 169, 043501 (2022).
3. H. Vogt and J. Thonstad, *Electrochim. Acta* 250, 393 (2017).
4. H. Vogel, B. Flerus, F. Stoffner, and B. Friedrich, *J. Sustain. Metall.* 3, 99 (2017).
5. B.P. Holcombe, N.S. Sinclair, R. Wasalathanthri, B. Mainali, E. Guarr, A.A. Baker, S.O. Usman, E. Kim, S. Sen-Britain, H. Jin, S.K. McCall, and R. Akolkar, *ACS Sustain. Chem. Eng.* <https://doi.org/10.1021/acssuschemeng.3c07720> (2024).
6. B.P. Holcombe, N.S. Sinclair, A.A. Baker, E. Kim, S.K. McCall, and R. Akolkar, *Electrochem. Soc. Interface* 33, 49 (2024).
7. R. Akolkar, B.P. Holcombe, N.S. Sinclair, R. Wasalathanthri. *Dimensionally stable anode for electrolytic chlorine evolution in molten salts*. Patent Application US20240158935A1 (2024).
8. N. Hildebrand, *Pogg. Ann.* 155, 631 (1875).
9. J. Shiokawa, T. Kurita, and T. Ishino, *J. Electrochem. Soc. Jpn.* 35, 7 (1967).
10. F. Trombe, *Trans. Electrochem. Soc.* 66, 57 (1934).
11. D. Sahoo, PhD thesis. Homi Bhabha National Institute, Trombay, India (2015).
12. D. Shen and R. Akolkar, *J. Electrochem. Soc.* 164, H5292 (2017).
13. M.F. Chambers, J. E. Murphy. U.S. Bureau of Mines. *Electrolytic production of neodymium metal from a molten chloride electrolyte*. (1991).
14. S. Im, N.D. Smith, S.C. Baldivieso, J. Gesualdi, Z.K. Liu, and H. Kim, *Electrochim. Acta* 425, 140655 (2022).
15. G.J. Janz, R.P.T. Tomkins. United States Department of Commerce - Bureau of Labor Statistics. *Physical Properties Data Compilations Relevant to Energy Storage. IV. Molten Salts: Data on Additional Single and Multi-Component Salt Systems*. (1981).
16. J.W. Yu and J.P. Wang, *Minerals* 14(5), 480 (2024).
17. K.T. Jacob, A. Dixit, and A. Rajput, *Bull. Mater. Sci.* 39(3), 603 (2016).
18. H. Mediaas, G. Photiadis, G.N. Papatheodorou, J.E. Vindstad, and T. Ostvold, *Acta Chem. Scand.* 51, 8 (1997).
19. R. Turton, J. Shawiwitz, D. Bhattacharyya, and W. Whiting, *Analysis, Synthesis, and Design of Chemical Processes*, 5th edn. (Prentice Hall, 2018).
20. D.R. Woods, *Rules of Thumb in Engineering Practice* (Wiley, 2007).
21. W.D. Seider, D.R. Lewin, J.D. Seader, S. Widagdo, R. Gani, and K.M. Ng, *Product and Process Design Principles: Synthesis, Analysis, and Evaluation* (Wiley, 2016).
22. G. Towler and R. Sinnott, *Chemical Engineering Design: Principles, Practice, and Economics of Plant and Process Design* (Butterworth-Heinemann, 2021).
23. D. Green and M. Southard, *Perry's Chemical Engineers' Handbook*, 9th edn. (McGraw Hill Education, 2019).
24. A. Mayyas, M. Ruth, B. Pivovar, G. Bender, K. Wipke. National Renewable Energy Laboratory. U.S. Department of Energy. Manufacturing Cost Analysis for Proton Exchange Membrane Water Electrolyzers. Office of Energy Efficiency & Renewable Energy (2019).
25. US Bureau of Labor Statistics. *May 2024 State Occupational Employment and Wage Estimates*. <https://www.bls.gov/oes/current/oesrcst.htm>. (2024).
26. E. Vahidi and F. Zhao, *J. Environ. Manag.* 203, 1 (2017).
27. D. K. Dysinger, J.E. Murphy, Electrowinning of neodymium from a molten oxide-fluoride electrolyte. Report of Investi-

- gations 9504; US Department of the Interior, Bureau of Mines (1994).
28. C. Liao, L. Que, Z. Fu, P. Deng, A. Li, X. Wang, and S. Chen, *Metals*. <https://doi.org/10.3390/met14040407> (2024).
  29. B.J. Welch, in *Hall-Héroult Centennial: First Century of Aluminum Process Technology*, ed by W.S. Peterson, R.E. Miller (TMS, 1986), p. 121.
  30. O. Wallevik, K. Amundsen, A. Faucher, T. Møllerud, in *Magnesium Technology 2000*, ed by H.I. Kaplan, J.N. Hryn, B.B. Clow (TMS, 2000) p. 93–96.
  31. M. Moeller. *Primary Magnesium Refining RTR Docket (Docket ID No. EPA-HQ-OAR-2020-0525)*. US Environmental Protection Agency: Primary Magnesium Refining: National Emissions Standards for Hazardous Air Pollutants (NESHAP). (2020).
  32. T.G. Tripp, *Nat. Resour. Environ. Issues* 15, 10 (2009).
  33. Y.V. Murty, M.A. Alvin, and J.P. Lifton, *Rare Earth Metals and Minerals Industries: Status and Prospects* (Springer, 2024).
  34. R. Keller and K.T. Larimer, *Final Report on Electrolysis of Neodymium Oxide* (US Department of Energy, 1997).
  35. A.H. Kheyriyeh, F. Ostovarpour, M. Khani, M.S.A. Shanbehbazari, and B. Shokri, *Heliyon*. <https://doi.org/10.1016/j.heliyon.2024.e41451> (2025).
  36. H. Vogel and B. Friedrich. *Light Metals 2018*. The Minerals, Metals & Materials Series. Springer (2018).
  37. MP Materials. <https://investors.mpmaterials.com/investor-news/news-details/2025/MP-Materials-Restores-U.S.-Rare-Earth-Magnet-Production/default.aspx>. (2025).
  38. H. Kvande, *Occup. Environ. Med.* 56(5S), S2 (2014).
  39. Energy Information Administration. <https://www.eia.gov/stata/data.php?sid=OH>. (2025).
  40. Shanghai Metals Market. <https://www.metal.com/Rare-Earth-Oxides/201102250592>. (2025).
  41. Alibaba. [https://www.alibaba.com/product-detail/Industrial-Feed-Grade-Calcium-Chloride-White\\_1601245626496.html](https://www.alibaba.com/product-detail/Industrial-Feed-Grade-Calcium-Chloride-White_1601245626496.html). (2025).

**Publisher's Note** Springer Nature remains neutral with regard to jurisdictional claims in published maps and institutional affiliations.